241

Adv. Space Res. Vol. 1, pp. 423-437.
©COSPAR, 1981. Printed in Great Britain.

0273-1177/81/0201-0423$05.00/0

POWER LINE RADIATION IN THE MAGNETOSPHERE

C. G. Park and R. A. Helliwell

Radioscience Laboratory, Stanford University, Stanford, California 94305, USA

ABSTRACT

VLF radiation from electrical power transmission lines stimulates nonlinear wave-particle and wave-wave interactions in the magnetosphere, resulting in wave growth, triggering of emissions, and entrainment of other natural or manmade VLF waves. Examples of these effects will be reviewed using both ground-based and satellite data. In many instances, the interpretation of data is aided by Siple transmitter results that show similar spectral characteristics.

INTRODUCTION

Power line radiation (PLR) in the magnetosphere has been discussed in many recent papers [1-16]. Harmonic radiation from electrical power transmission lines in the range of a few kHz leaks into the magnetosphere and stimulates a coherent wave instability, resulting in strong amplification of the input waves and the generation of free-running emissions. These amplified waves and associated emissions cause pitch angle scattering of trapped energetic electrons, some of which enter the loss cone and are absorbed in the atmosphere. Although there seems to be no disagreement about the existence of the PLR phenomenon, the overall importance of its effects on the wave and particle environment in the magnetosphere is far from being clear.

Observations to date indicate that PLR waves entering the magnetosphere from below are too weak to directly affect the dynamics of energetic particles. On the other hand, magnetospherically amplified PLR waves and PLR-triggered emissions are of sufficient intensity to significantly affect the lifetime of trapped energetic electrons [1,17]. Thus, an understanding of the amplification and triggering processes is central to understanding the role of PLR in magnetospheric dynamics. Owing to the nonlinear nature of these processes, however, the resulting waves show many complex spectral features that are not well understood at present, and it is often difficult to associate the amplified or triggered waves with the weak input waves.

In this paper we present some recent observational results that provide new information on the PLR phenomenon. These results will be prefaced by a brief review of past work whenever appropriate. However, it is emphasized that this paper is not intended as a comprehensive review of the PLR phenomenon.

EXAMPLES OF MAGNETOSPHERIC LINE RADIATION

Magnetospheric line radiation appears in a variety of spectral forms. In this section we show some clear examples of magnetospheric line radiation associated with PLR. Figure 1 shows simultaneous spectrograms from a conjugate pair of stations, Roberval, Quebec (48°N, 73°W) and Siple, Antarctica (76°S, 84°W). The Roberval record shows two sets of horizontal lines. The sharp lines, spaced exactly 120 Hz apart, are local interference or induction lines at odd multiples of the local 60 Hz power line frequency. The other set of lines, somewhat broader and displaced by ~20-30 Hz above the local induction lines, are called "magnetospheric lines" and are observed at both Roberval and Siple. An amplitude modulation with a 3-sec periodicity is apparent at both stations. This AM period is the two-hop whistler-mode echo period and thus provides clear evidence that the waves propagated through the magnetosphere. The frequency shift of magnetospheric lines with respect to local induction lines is a commonly observed feature and will be discussed in a later section.

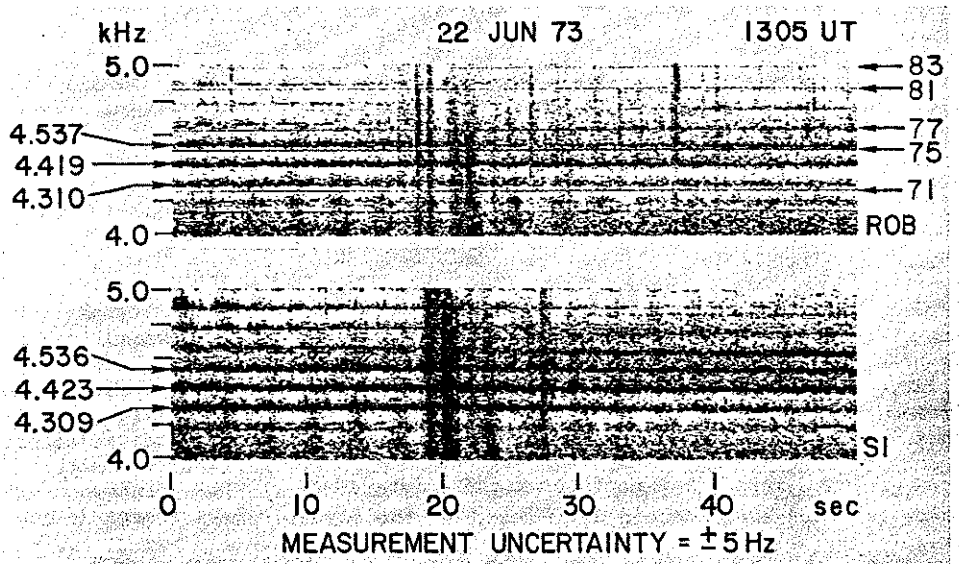

Fig. 1 Simultaneous conjugate recording from Roberval and Siple showing magnetospheric line radiation. The numbers on the left indicate the center frequency of magnetospheric lines, while the numbers on the right-hand side of the Roberval record are the harmonic numbers of the local induction line. (From Helliwell et al. [1].)

Figure 2 shows two more examples of PLR events recorded at Eights, Antarctica (75°S, 77°W). The top panel clearly shows strong amplitude modulation at the whistler-mode echo frequency. Many of the lines show considerable frequency broadening but their center frequencies remain roughly constant. In the bottom panel, the line radiation triggers rising tone emissions that cross adjacent

lines and merge to form broadband noise bursts.

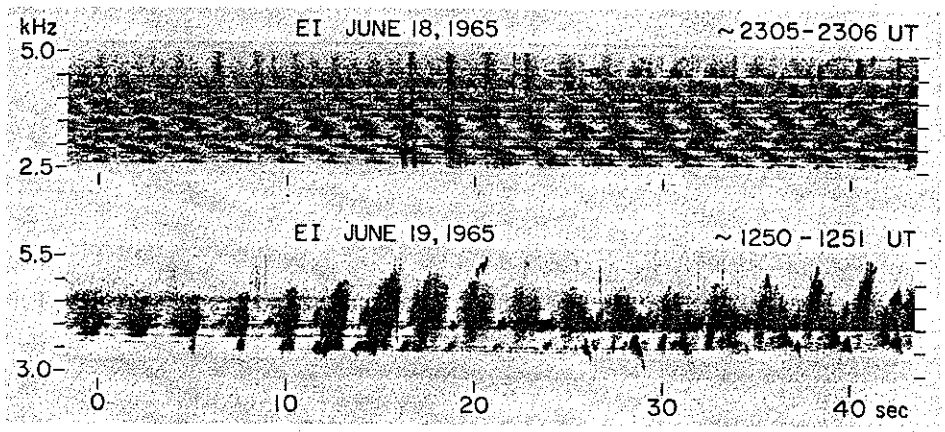

Fig. 2 Two examples of PLR-induced magnetospheric emissions recorded at Eights, Antarctica. (From Park [4].)

Figure 3 shows another example of simultaneous conjugate recordings from Siple and Roberval. The conjugacy and amplitude modulation are quite apparent. In this example, many of the modulated magnetospheric lines can be seen to coincide with local induction lines at Roberval.

PLR can affect the behavior of other emissions by entraining them or cutting them off [18,1]. There is also evidence that magnetospheric PLR events can be stimulated by other waves such as whistlers and VLF transmitter signals.

Figures 4 and 5 show examples of long-enduring bursts of emissions, apparently triggered by whistlers. In Figure 4, multiple line radiation lasting for more than 4 min can be traced back to a whistler at $t \cong 40$ sec. Short segments of echoing wave packets near the beginning of this event show how they are amplified during successive passes through the magnetosphere. They are not even discernable until they have passed several times through the magnetosphere, but once they reach a certain threshold they trigger emissions, which in turn appear to stimulate adjacent lines. The falling tone emission at $t \cong 1$ min 40 sec echoes and "turns on" line radiation in a manner similar to the whistler at $t = 40$ sec.

Figure 5 shows an event similar to that of Figure 4. The vertical arrows mark the two-hop whistler echo period at 3.78 kHz where the PLR starts to grow. The top panel shows the amplitude record corresponding to the first spectrogram. Further details of the events in Figures 4 and 5, as well as a similar event stimulated by VLF transmitter signals, will be given in a separate paper [19].

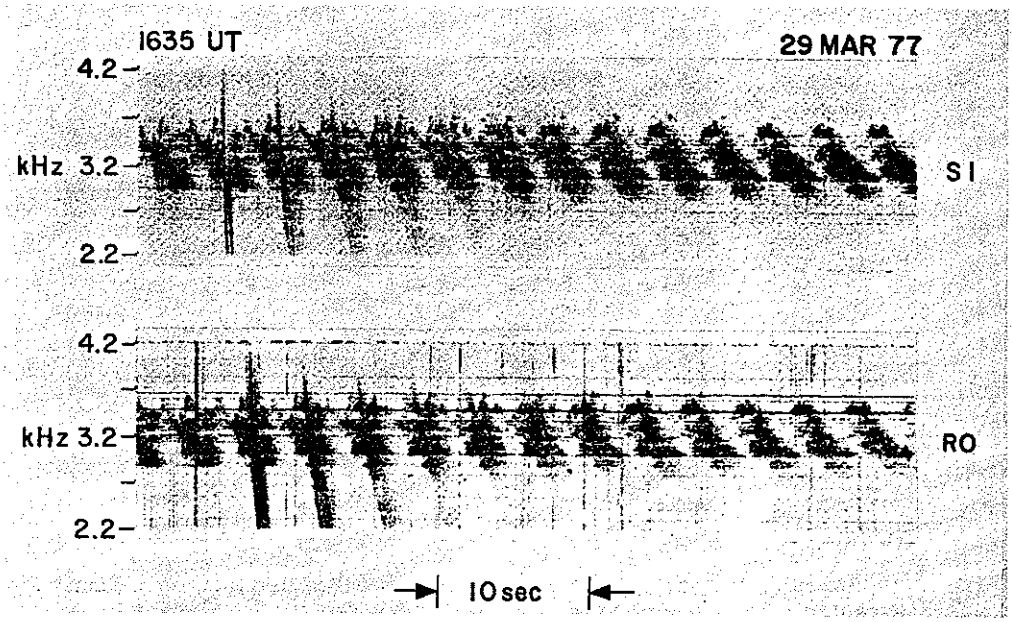

Fig. 3 Conjugate recordings at Siple and Roberval showing PLR-induced emissions with strong amplitude modulation at the whistler-mode bounce frequency.

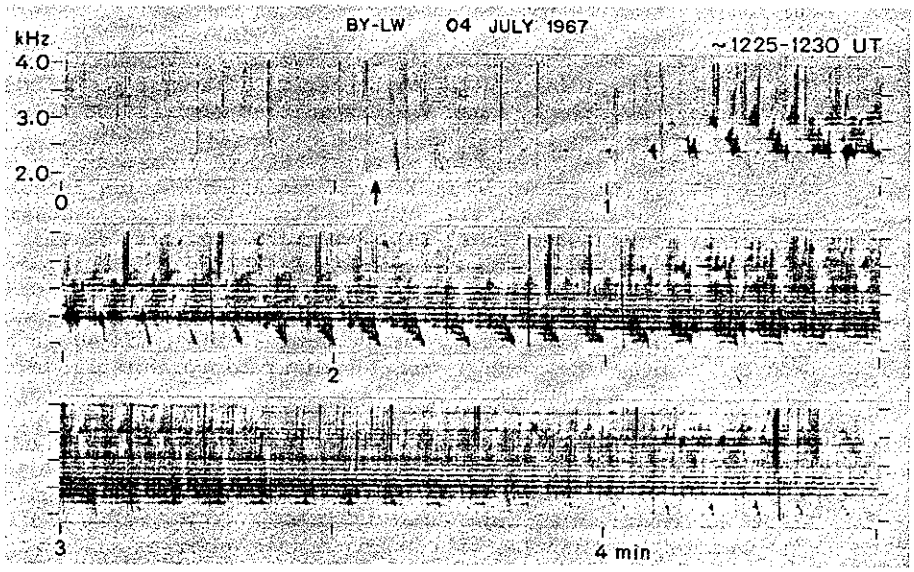

Fig. 4 An example of long-enduring burst of line radiation recorded at Byrd, Antarctica, using a 21-km long dipole antenna.

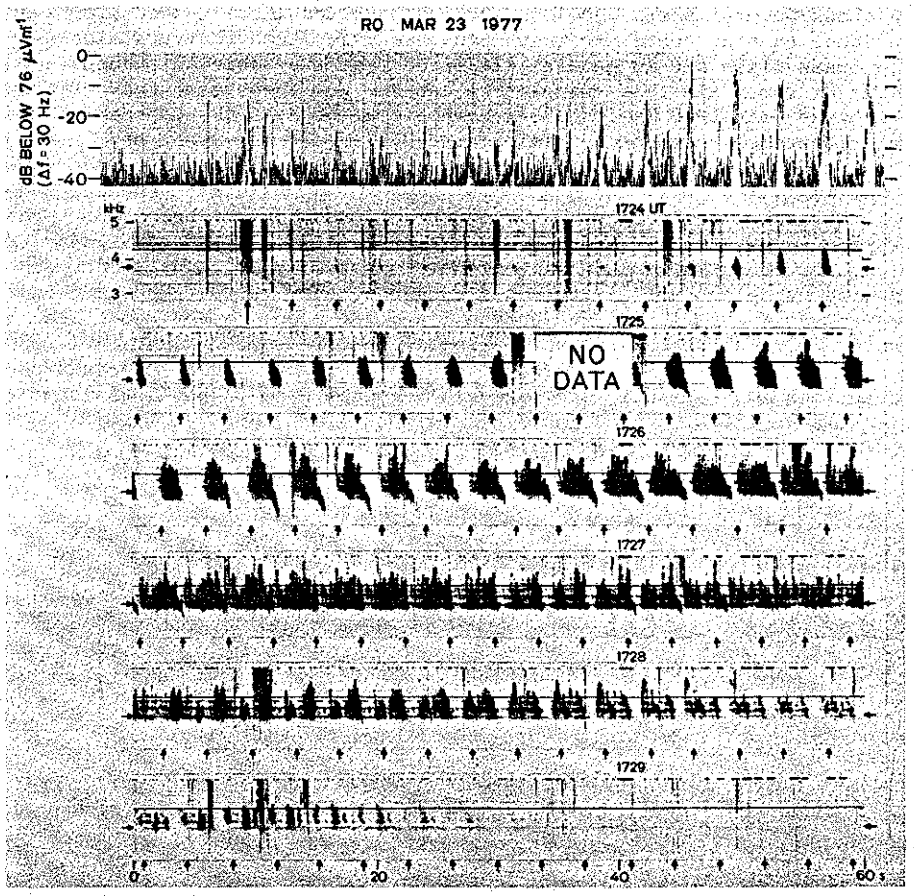

Fig. 5 A 6-min recording from Roberval showing a burst of line radiation and associated emissions, apparently initiated by a whistler-PLR interaction. The vertical arrows indicate the two-hop whistler bounce time, while the horizontal arrows mark 3780 Hz where the burst event starts. The top panel shows the wave amplitude at 3780 ± 15 Hz, corresponding to the spectrogram directly below.

FREQUENCY OFFSET

As noted above, magnetospheric line radiation sometimes appears at frequencies measurably different from exact power line harmonic frequencies. They may also show frequency spacings of only 20-30 Hz in regions where the fundamental power line frequency is 60 Hz or 50 Hz [1,16]. Such frequency offset is most likely to be the result of nonlinear amplification in the magnetosphere, as evidenced by the similar behavior of VLF transmitter signals injected into the magnetosphere. Several examples below illustrate how frequency offsets of PLR and transmitter signals develop.

Figure 6 shows simultaneous recordings from Roberval and Siple. The Roberval record shows several sharp local odd-order induction lines spaced 120 Hz apart. Also evident on the record are many magnetospheric lines that are also seen at Siple. These lines are in general displaced from the Roberval induction lines by ~10 Hz or more. In this example, we can see how these frequency offsets develop in time. At 1980 Hz (the 33rd harmonic of 60 Hz), the magnetospheric line at Siple starts to become intensified at t ≈ 17 sec. Then, one hop later, the first evidence of intensification is seen at Roberval. This means that when PLR was first amplified, only the southward propagating PLR was amplified, suggesting that the PLR echo propagating in the opposite direction was below the threshold for temporal growth [20]. At t = 18.5 sec, a short enhancement is identified at Siple and marked by arrow 1. This intensified wave packet echoes many times through the magnetosphere as indicated by subsequent arrows. Echo 2 coincides in frequency with the 1980 Hz induction line, but echo 4 has a short line segment about 20 Hz above the induction line. There is some indication in the Siple record that this new frequency component was generated at the third echo. Subsequent echoes show additional frequency components. A particularly clear example is echo 12, with two line segments above the induction line.

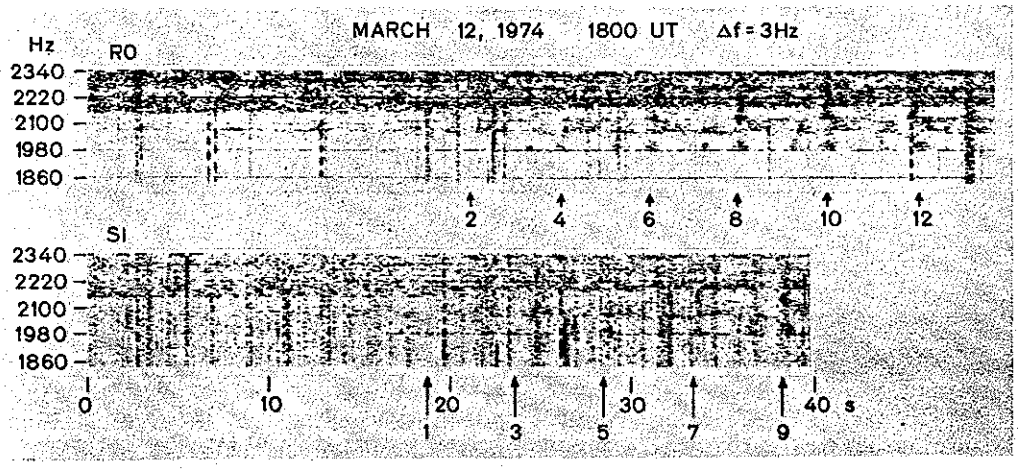

Fig. 6 Simultaneous spectrograms for Roberval and Siple illustrating the development of fine structures in line radiation apparently stimulated by PLR at Roberval.

Echoing transmitter pulses also show a tendency to drift in frequency, as illustrated in Figure 7. This spectrogram from Siple shows two 2-sec transmitter pulses starting at t = 0 and t = 10 sec. During these transmit times, the receiver gain is reduced to avoid saturation, and as a result, all weak waves are blanked out. About 5.5 sec following each pulse, a two-hop echo is seen with considerable frequency broadening and triggered emissions. The four-hop echo arrives ~11 sec after transmission and partially overlaps the next transmitter pulse. It is evident that the four-hop echoes have been shifted up by ~20 Hz from the original transmitter frequency. A possible explanation of such a frequency shift is that when a monochromatic pulse is amplified, its spectrum is usually broadened but more on the high frequency side than on the low frequency

side so as to shift the center frequency upward [21].

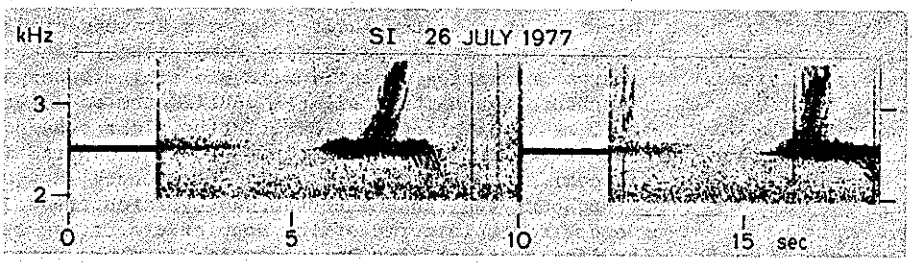

Fig. 7 Echoes of Siple transmitter signals showing the tendency for upward frequency shift. See text for details.

Figure 8 shows another example from Siple transmitter signals observed at Roberval. The transmitted signal was a single constant amplitude sinusoidal wave at 4870 Hz. The magnetospheric output shows many sidebands spaced ~20-30 Hz apart. Upper sidebands are more prominent than lower sidebands, and the sidebands as well as the carrier are strongly amplitude-modulated at ~2 Hz. We suggest that similar sideband generation may accompany amplified PLR and may explain some of the line radiation with spacings less than the fundamental power line frequency.

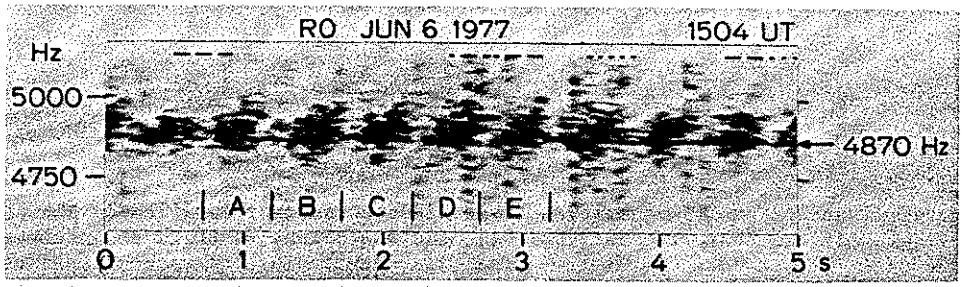

Fig. 8 An example of side bands generated by the Siple transmitter and received at Roberval. (From Park [29].)

SATELLITE OBSERVATIONS

Line radiation has also been observed on satellites over a wide range of altitude. Its properties are broadly similar to PLR-induced line radiation observed on the ground, including frequency shift and broadening. However, satellite data exhibit additional complications arising from satellite motion (i.e., Doppler shift) and from the fact that satellite receivers in general have a limited dynamic range. This limitation makes it difficult to detect weak-input PLR waves in the presence of other strong waves. For these reasons, reports of direct satellite observations of PLR effects have been slow to emerge. In this section we show some examples of line radiation observed on satellites that is tentatively

attributed to PLR.

Figure 9 shows an example of line radiation observed on the ISIS 2 satellite over North America. Several lines appear between 1 kHz and 1.8 kHz, but their spacing is irregular and varies with time. This behavior can be attributed at least in part to the Doppler shift which can be appreciable if the waves are unducted and have large wave normal angles with respect to the static geomagnetic field (i.e., large refractive index). Evidence of large Doppler shifts comes from observations of Siple transmitter signals onboard the same satellite, as illustrated in Figure 10. The top panel of Figure 10 shows the transmitter format, while the bottom panel shows the signal as received by the satellite. The "key-down" portion of the signal shows the transmitted frequency at 5.05 kHz; in addition, a range of frequencies extending to ±80 Hz about the transmitted frequency is observed. In order to explain these frequency shifts in terms of the Doppler effect, we require multiple unducted paths. Assuming that the wave normal vector is nearly parallel or antiparallel to the satellite velocity vector, we find that the magnitude of the refractive index must be about 700, which is an acceptable figure for large wave normal angles with respect to the static magnetic field.

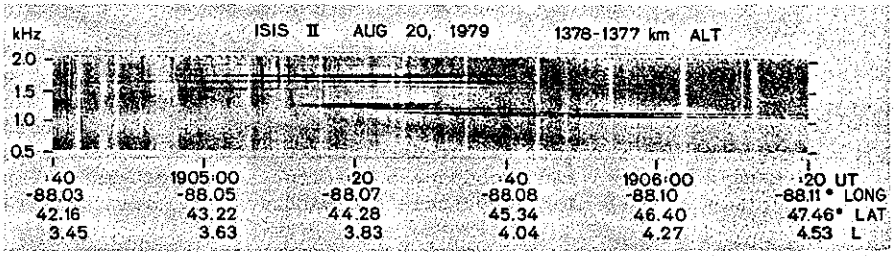

Fig. 9 An example of magnetospheric line radiation observed onboard the ISIS 2 satellite.

Figures 11 and 12 show further examples of PLR detected by the ISIS 2 satellite. In Figure 11, the sharp line at 60 Hz is modulated at one-half the satellite spin period (20 sec), evidence that the signal was detected by the spacecraft antenna, and not introduced by ground instruments. The essentially monochromatic appearance suggests that the signal reached the satellite directly from a ground source. The intensity of the 60-Hz signal was comparable to that of simultaneous NAA transmitter signals at 17.8 kHz. This transmitter radiates 1 MW power from Cutler, Maine, approximately 500 km from the satellite ground track (absolute intensity determination requires detailed analysis of the receiver gain state, which was controlled by the onboard automatic gain control system. Such analysis is now underway, and the results will be reported later.).

Figure 12 shows an example of line radiation at 180 Hz. Its characteristics are similar to those of the 60 Hz lines in Figure 11. In this case, however, there is only a hint of 60 Hz signal.

Figure 13 shows an example of line radiation detected by a high-altitude satellite, ISEE 1. A portion of the top panel marked AA' is reproduced below. The vertical striations in both panels are due to spacecraft spin modulation. The

labeled horizontal lines are at multiples of 60 Hz. Line radiation similar to that of Figure 13 is observed by the ISEE satellite in approximately 5% of the orbits covering L ≅ 4-8 in the American longitude sector. Observed line radiation tends to occur when the receiver gain happens to be relatively high because of the absence of other competing strong waves [22]. In other cases examined by Bell et al. [22], the line radiation frequencies deviate significantly from the power line harmonic (PLH) frequencies, as we have seen in both the ground data and low-altitude satellite data.

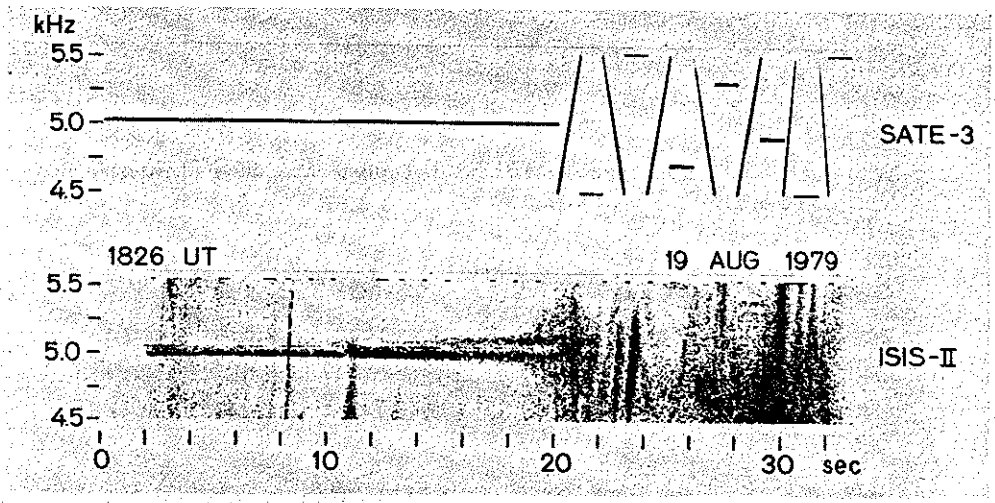

Fig. 10 (Top) The signal modulation format transmitted from Siple. (Bottom) The same signal received by the ISIS 2 satellite traveling northward near the conjugate point of Siple. The satellite position at 1826 UT was 39°N, 77°W, 1380 km altitude, L = 3.1.

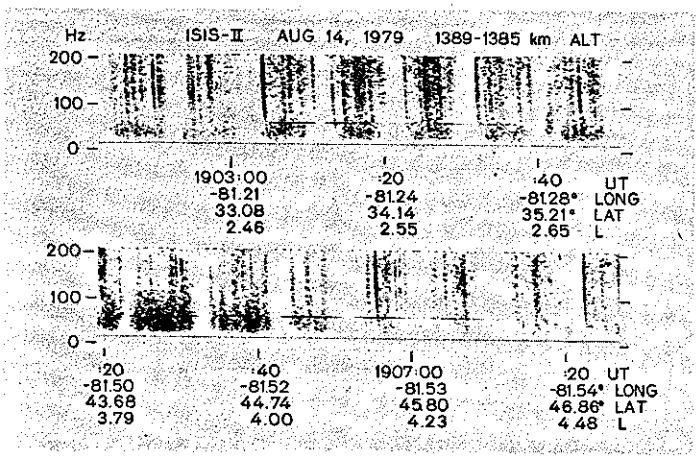

Fig. 11 ISIS 2 satellite data showing a constant frequency signal at 60 Hz. The intensity modulation at 10-sec period is due to the satellite spin.

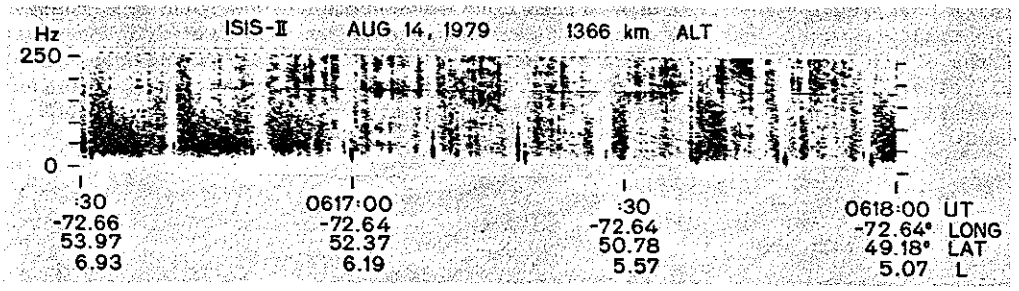

Fig. 12 ISIS 2 satellite data showing a monochromatic signal at 180 Hz.

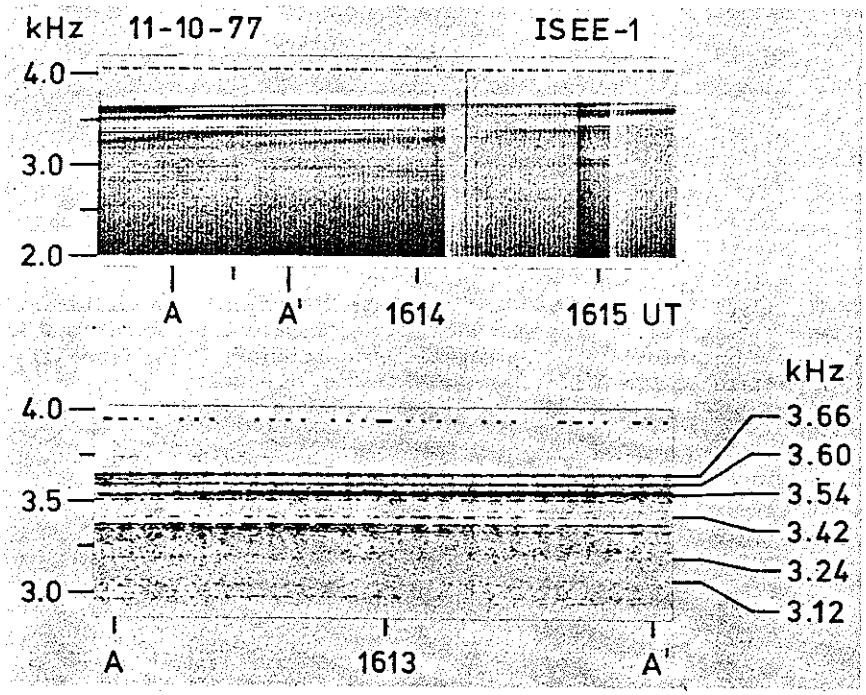

Fig. 13 An example of line radiation observed onboard the ISEE 1 satellite. The satellite location was 45°W geographic longitude, 8°N geomagnetic latitude, L ~ 5.2. (From Bell et al. [22].)

CHORUS STARTING FREQUENCY

Some chorus elements show well-defined starting frequencies, as illustrated in Figure 14. Luette et al. [12] reported that the majority of the measured starting frequencies of such chorus elements in the OGO 3 VLF spectra were within ±2 Hz of the PLH frequencies. This was interpreted as evidence that these chorus elements were triggered by PLR.

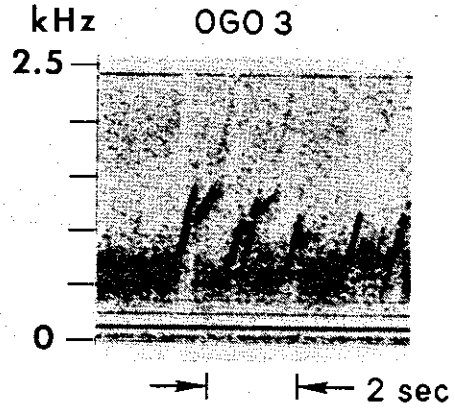

Fig. 14 An example of OGO 3 satellite data showing chorus elements with exceptionally well-defined starting frequency. (From Luette et al. [12].)

It should be noted that the starting frequency can be identified and measured in only a small fraction (~10%) of all observed chorus [12]. In the majority of cases, the starting frequency cannot be identified with less than 50 Hz uncertainty. This, however, is not inconsistent with the behavior of triggered emissions. Emissions triggered by transmitter signals often appear with no direct connection to the triggering signal. An example of such behavior is illustrated in Figure 15. When we compare the Roberval spectrogram with the Siple transmitter format shown below, it is clear that most of the emissions seen at Roberval were triggered by the transmitter. Yet it is not possible to identify monochromatic signals in the Roberval data. This is in sharp contrast to another class of phenomena where the input signal remains essentially monochromatic during early stages of amplification [18,21]. Satellite observations onboard ISEE 1, EXOS B and ISIS show that the emissions triggered by nonducted transmitter signals exhibit spectral characteristics similar to those illustrated in Figure 16. In particular, they are not preceded by monochromatic triggering signals [23,24].

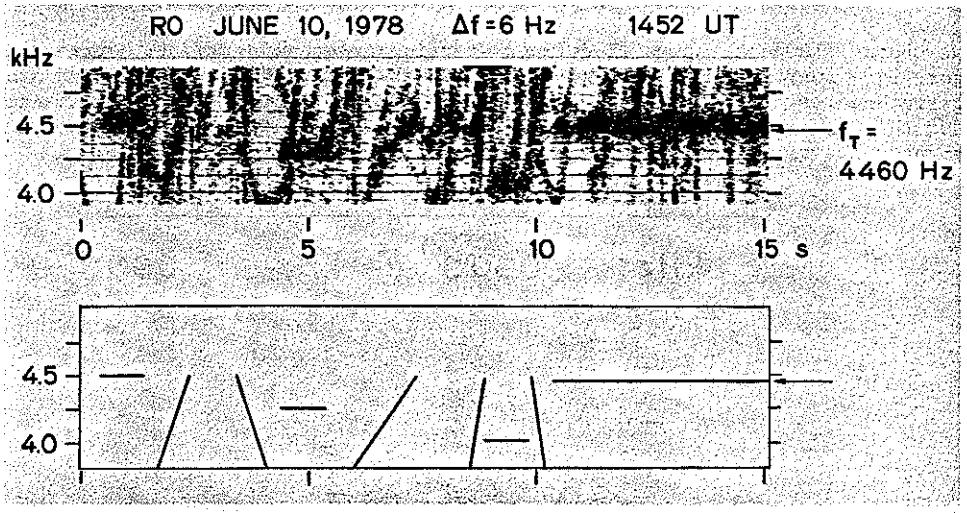

Fig. 15 (Top) Emissions stimulated by the Siple transmitter and received at Roberval. (Bottom) The Siple transmitter format.

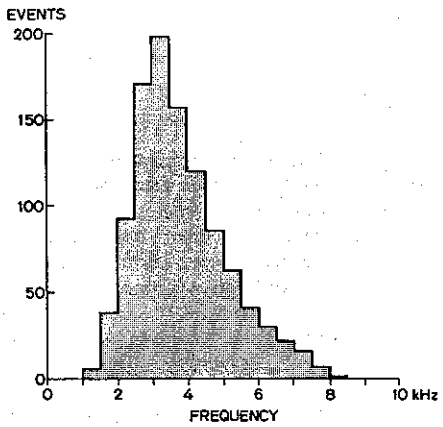

Fig. 16 The frequency distributions of PLR-induced emissions observed at Siple and Eights, Antarctica. (From Park and Helliwell [7].)

DISCUSSION AND CONCLUDING REMARKS

Magnetospheric line radiation has been observed both on the ground and on satellites. The observed spectra, particularly in the case of satellite observations, show many complex features such as frequency shifts and broadening that evidently arise from nonlinear wave-particle interactions and propagation effects in the magnetosphere. Similar features are also observed in controlled wave-injection experiments using the Siple VLF transmitter. Some transmitter experiments have shown that PLR effects can be simulated with as little as 0.5 W radiated power at a given frequency [8].

Ground observations of PLR effects have thus far been limited to the American longitude sector where strong PLR sources are known to be present. Future observations at other longitudes where PLR sources are absent or weak could clarify some of the unanswered questions about PLR effects.

Satellite data have been used to study the geographical distribution of wave activity that could be related to PLR sources on the ground. The results to date, however, are inconclusive. VLF data from OGO 3 [6] as well as Ariel 3 and 4 [25, 2,13] showed enhanced wave activity over industrialized areas of the world, which was attributed to stimulation by PLR. On the other hand, ELF data from OGO 5 and 6 showed no significant geographical variations that could be linked to PLR [10, 11]. This difference could be due to the limited frequency coverage of OGO 5 and OGO 6 instruments. PLR effects as observed on the ground occur in a limited frequency range, as shown in Figure 16. OGO 5 and 6 instruments, covering a frequency range of 10 Hz to 1 kHz [26] are not expected to observe many PLR events. Ariel satellite results cited above also show that the zones of enhanced activity become obscured at these low frequencies.

Little is known about PLR sources. More measurements are needed to learn about their intensity as a function of frequency, their geographical distribution and temporal variations. Recent observations by Hayashi et al. [27] and Akasofu and Merritt [28] indicate that ionospheric currents during geomagnetic disturbances can induce large quasi-DC currents in power lines. These currents tend to cause saturation in transformer cores, which in turn can increase the harmonic content of the AC power.

In summary, PLR stimulates many subtle and complex wave-particle interactions in the magnetosphere that are similar to those simulated by controlled transmitter signals. These interactions undoubtedly affect both wave and particle environments in the magnetosphere; however, a quantitative assessment of their importance, vis-a-vis naturally occurring phenomena, is not possible until further information becomes available.

ACKNOWLEDGMENTS

We thank J. G. James of the National Research Council, Canada, for providing the ISIS VLF data used in this paper and J. P. Katsufrakis of our laboratory for calling our attention to interesting ISIS PLR events in both the ISIS and ground-based data. We also thank J. Yarborough, B. M. Blockley and K. Dean for their help in preparing the illustrations and producing the camera-ready typescript. This work was supported by the National Science Foundation, Atmospheric Sciences Section, under grant ATM78-20967, by the National Science Foundation, Division of Polar Programs, under grant DPP76-82646, and by the National Aeronautical and Space Administration under grants NAS5-25744 and NGL-05-020-008.

REFERENCES

1. R. A. Helliwell, J. P. Katsufrakis, T. F. Bell, and R. Raghuram, J. Geophys. Res. 80, 4249 (1975).

2. K. Bullough, A. R. L. Tatnall, and M. Denby, Nature 260, 401 (1976).

3. C. G. Park, in: Physics of Solar Planetary Environments, AGU, Washington, D. C., 1976.

4. C. G. Park, J. Geophys. Res. 82, 3251 (1977).

5. C. G. Park and R. A. Helliwell, J. Geophys. Res. 82, 3634 (1977).

6. J. P. Luette, C. G. Park, and R. A. Helliwell, Geophys. Res. Lett. 4, 275 (1977).

7. C. G. Park and R. A. Helliwell, Science 200, 727 (1978).

8. C. G. Park and D. C. D. Chang, Geophys. Res. Lett. 5, 861 (1978).

9. H. C. Koons, M. H. Dazey, and B. C. Edgar, J. Geophys. Res. 83, 3887 (1978).

10. R. M. Thorne and B. T. Tsurutani, Science 204, 839 (1979).

11. B. T. Tsurutani, S. R. Church, and R. M. Thorne, J. Geophys. Res. 84, 4116, (1979).

12. J. P. Luette, C. G. Park, and R. A. Helliwell, J. Geophys. Res. 84, 2657 (1979).

13. K. Bullough and T. R. Kaiser, in: Wave Instabilities in Space Plasmas, Reidel, Dordrecht, 1979.

14. C. G. Park and T. R. Miller, J. Geophys. Res. 84, 943 (1979).

15. R. A. Helliwell, in: Wave Instabilities in Space Plasmas, Reidel, Dordrecht, 1979.

16. J. P. Matthews and K. Yearby, Planet. Space Sci. (in press) (1980).

17. A. R. L. Tatnall, J. P. Matthews, K. Bullough, and T. R. Kaiser, Scientific Report 1978 No. 1, Space Physics Group, University of Sheffield, South Yorkshire, U. K., 1978.

18. R. A. Helliwell and J. P. Katsufrakis, J. Geophys. Res. 79, 2511 (1974).

19. C. G. Park and D. L. Carpenter, J. Geophys. Res. (in press) (1980).

20. R. A. Helliwell, D. L. Carpenter, and T. R. Miller, J. Geophys. Res. (in press) (1980).

21. G. S. Stiles and R. A. Helliwell, J. Geophys. Res. 80, 608 (1975).

22. T. F. Bell, J. P. Luette, and U. S. Inan, J. Geophys. Res. (in press) (1980).

23. T. F. Bell, U. S. Inan, and R. A. Helliwell, J. Geophys. Res. (in press) (1980).